Continuum mechanics of apical constriction

Marija Krstić and Pierre Haas

Abstract

The goal of the project is examining different regimes in the folding of a cell sheet as a consequence of applied compression to the sides of the cell sheet. First, a theoretical continuum model is derived from a discrete one based on the geometry of the system with differing basic assumptions about the shape of the cells during the folding of the cell sheet. Afterwards, using the continuous variables introduced to describe the continuum model, the condition for buckling and self-intersection of the cell sheet is investigated to analyse the geometric singularity of apical constriction, i.e. the regime relevant for developmental biology in which cells become triangular and hence maximally bent.

Dresden
26.10.2022.

1 Introduction

The folding of an epithelial cell sheet gives rise to the formation of many organs and has often been studied using the model of gastrulation of embryos. This has led to a number of studies trying to explain the process of folding as well as to predict the shape of the folds that appeared, such as Ref. [1]. Although various approaches to the problem have been developed, the model we will be using is the differential-tension model. This model is based on the idea that there are different surface tensions on the sides of the cells as a consequence of certain properties of the cell (e.g. its polarity, adhesion properties, etc.). In this paper, we seek to explain the buckling process of a monolayer of epithelial cells by deriving a continuum theory from a discrete, geometric model based on the shape of individual cells during the folding process.

2 Modelling the buckling

Two different models are used in order to try and explain the folding process of a cell sheet. In the first one, the initial assumption is that during the folding of the cell sheet, the individual cells fold to form isosceles trapezoids, which have only one degree of freedom because of the fact that the lateral sides of the cells are of the same length as the cells are connected to each other along the lateral sides. In the second model, the first assumption is relaxed so that individual cells are described as non-isosceles trapezoids that now have two degrees of freedom each.

2.1 Isosceles model

As mentioned above, the first model is derived with the assumption that individual cells can be described as isosceles trapezoids during the folding process. Following Ref. [2], we firstly introduce ϕ as a variable that describes the state of the individual cell, which is depicted in Fig. 1.

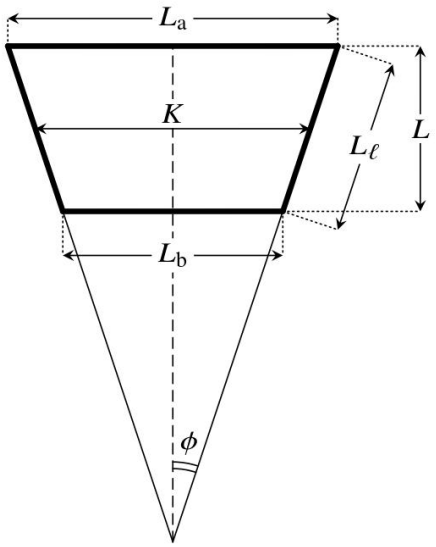

Figure 1: Description of the system at the cell level. Taken from Ref. [2].

Since ϕ is a parameter describing the cells, in order to establish a continuum theory of the buckling process, a new variable is introduced: the angle ψ that the midline of the cell sheet forms with the horizontal, as can be seen in Fig. 2.

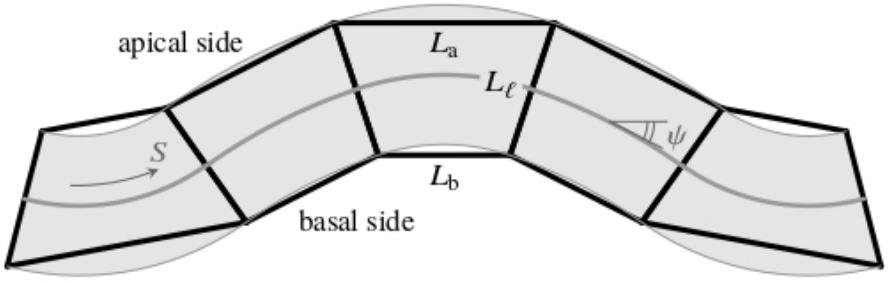

Figure 2: Description of the system at the cell sheet level as a continuum. Taken from Ref. [2].

The goal is to describe the state of the cell sheet through the variable ψ when compression is introduced to the sides of the cell sheet. We will see that three main regimes can be spotted during the increase of the compression, with critical values which we will from now on refer to as D_* and $D_\triangle$, respectively. For $0 < D < D_*$ the cell sheet does not fold, but responds to the compression by increasing the thickness of the cell sheet while maintaining $\psi = 0$. The critical value of the compression is D_* at which the cell sheet begins to fold. The folding continues up until $D_\triangle$ when individual cells at some parts of the sheet cannot fold any further, for they have reached a triangular shape, so further folding would cause the sides of the cell to self-intersect which cannot happen in the biological system. In the following paragraphs a differential equation describing the angle ψ will be derived and solved analytically for small compressions near the buckling threshold D_* and numerically for larger compressions.

2.1.1 Continuum model

Following Ref. [2], the description of the model starts with defining the energy of a single cell. Since a differential-tension model is assumed, different surface tensions are established at the apical, basal and lateral side of the cells, labeled with Γ_a, Γ_b, and Γ_l respectively. Furthermore, the epithelium is described as a two-dimensional model which consists of isosceles trapezoids linked by their lateral sides of length L_l, with parallel apical and basal sides of lengths L_a and L_b shown in Figs. 1 and 2. This gives us the energy of a single cell,

$$E = \Gamma_a L_a + \Gamma_b L_b + \Gamma_l L_l.$$

From the geometry of the isosceles trapezoid, it is possible to express the lengths of the sides of the cell as a function of the angle ϕ, the mean base K and the height L as per the notation used in Fig 1,

$$\begin{aligned} L_a &= K + L_l \sin\phi, \\ L_b &= K - L_l \sin\phi, \\ L &= L_l \cos\phi. \end{aligned}$$

During the folding, it is assumed that the cells are incompressible, meaning that the cell area $A_c = KL$ is conserved. Using these identities, the energy of the cell can now be defined as a function of L_l and ϕ as

$$E = (\Gamma_a + \Gamma_b)\frac{A_c}{L_l}\sec\phi + (\Gamma_a - \Gamma_b)L_l \sin\phi + \Gamma_l L_l.$$

In the next step, nondimensionalization of the energy is performed by scaling lengths of the cell sides with the square root of the area of the cell, introducing

$$\lambda = \frac{L_l}{\sqrt{A_c}}, \quad l = \frac{L}{\sqrt{A_c}}, \quad \kappa = \frac{K}{\sqrt{A_c}}.$$

Also, it will be useful to introduce the parameters

$$l_0 = \sqrt{\frac{\Gamma_a + \Gamma_b}{\Gamma_l}}, \quad \delta = \frac{\Gamma_a - \Gamma_b}{\Gamma_l},$$

so that l_0 is the thickness of the cell sheet in the unbuckled state. Another useful variable will be $s_0 = \frac{1}{l_0}$, which is the width of a single cell in the unbuckled state. Now, we can introduce the nondimensional energy as

$$e = \frac{E}{\Gamma_l \sqrt{A_c}} = \frac{l_0^2}{\lambda} \sec\phi + \lambda(\delta \sin\phi + 1).$$

Moving on to the continuum limit, the energy of the entire cell sheet is the integral of the energy of a single cell,

$$\epsilon = \int e(\phi) l_0 \, \mathrm{d}s = l_0^2 \int \left\{ \frac{l_0}{\lambda} \sec\phi + \frac{\lambda}{l_0}(\delta \sin\phi + 1) \right\} \mathrm{d}s.$$

For the complete transition to the continuum theory, it is necessary to express $\phi(s)$ as a function of $\psi(s)$, which can be derived from the geometry of the system. The details of this calculation can be found in Ref. [2]; here we will just present the final expression for $\phi(s)$,

$$\phi(s) = \frac{\psi'(s)}{2l_0} - \frac{\psi'''(s)}{24l_0^3} + \frac{\psi^{(v)}}{240l_0^5} + \cdots. \tag{1}$$

Additionally, we describe the folding of the epithelium by introducing a coordinate system ($x(s)$,$y(s)$) as in Fig. 3.

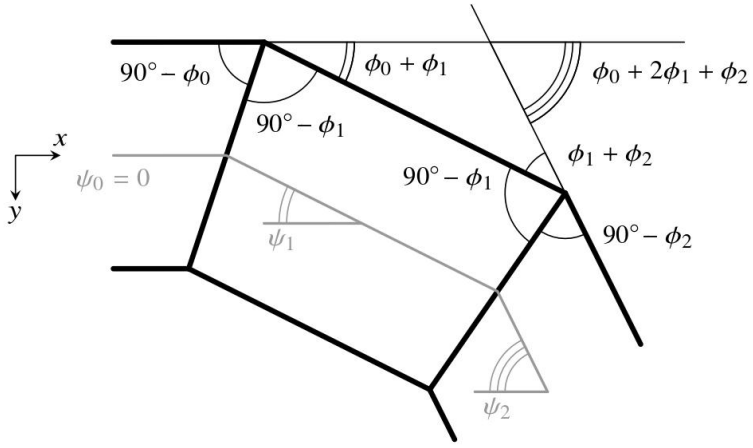

Figure 3: Geometry of neighbouring cells. Taken from Ref. [2].

Thence we can obtain the coordinates using the expressions

$$x(s+s_0) - x(s) = \frac{1}{2}\left[\kappa(s)\cos\psi(s) + \kappa(s+s_0)\cos\psi(s+s_0)\right],$$
$$y(s+s_0) - y(s) = \frac{1}{2}\left[\kappa(s)\sin\psi(s) + \kappa(s+s_0)\sin\psi(s+s_0)\right].$$

Expanding these equations using $\kappa(s) = \frac{1}{l_0\Lambda}\sec\phi(s)$, one gets, as derived in Ref. [2],

$$\Lambda \frac{\mathrm{d}x}{\mathrm{d}s} = f\cos\psi(s) - g\sin\psi(s), \tag{2}$$
$$\Lambda \frac{\mathrm{d}y}{\mathrm{d}s} = f\sin\psi(s) - g\cos\psi(s), \tag{3}$$

where

$$f = 1 + \frac{\psi'^2}{24l_0^2} + \frac{7\psi'^4 + 144\psi''^2 + 32\psi'\psi''}{5760l_0^4} + O(l_0^{-6}),$$
$$g = \frac{\psi''}{12l_0^2} + \frac{87\psi'^2\psi'' - 2\psi^{(iv)}}{1440l_0^4} + O(l_0^{-6}).$$

2.1.2 Deriving the governing equation

We will examine the conditions for buckling of a cell sheet whose undeformed length is $2\Sigma \gg s_0$. For this purpose, we will introduce a new variable $\sigma = \frac{s}{\Sigma} \in [0, 2]$ and denote the derivative with respect to σ with dots in the subsequent analysis. We will also define $\Xi = l_0\Sigma$, so that the number of the cells in the sheet can be easily defined as $N = 2\Xi$.

We are looking for buckled solutions with clamped boundary conditions and relative compression D, which satisfy the following conditions in terms of the new variable σ:

$$x(2) - x(0) = 2(1 - D), \qquad y(2) = y(0).$$

Also, we will restrict the solutions to symmetric ones, which yields the condition $\psi(\sigma) = -\psi(2 - \sigma)$. This already satisfies the condition imposed on y. Since we assume the buckled solution to be symmetric, we will reduce the range of σ to $\sigma \in [0, 1]$, with the first boundary condition above becoming $x(1)-x(0) = 1-D$. In order to minimize the energy of the buckled cells, we introduce the Lagrangian

$$\mathcal{L} = \int_0^1 \left\{ \frac{1}{\Lambda} \sec\phi(\sigma) + \Lambda(\delta \sin\phi(\sigma) + 1) \right\} \mathrm{d}\sigma + \frac{\mu}{\Sigma} \int_0^1 \dot{x}(\sigma)\, \mathrm{d}\sigma,$$

where μ is introduced as a Lagrange multiplier which can be interpreted as a horizontal compressive force. Using the expansion of ϕ given in Eq. (1), the Lagrangian becomes

$$\begin{aligned}\mathcal{L} = \int_0^1 \left(\Lambda + \frac{1}{\Lambda} + \frac{\dot{\psi}^2}{8\Lambda\Xi^2} - \frac{\delta\Lambda\dot{\psi}^3}{48\Xi^3} + \frac{5\dot{\psi}^4}{384\Lambda\Xi^4} + \frac{\ddot{\psi}^2}{48\Lambda\Xi^4} \right) \mathrm{d}\sigma \\ + \int_0^1 \frac{\mu\cos\psi}{\Lambda} \left(1 + \frac{\dot{\psi}^2}{8\Xi^2} + \frac{41\dot{\psi}^4}{1920\Xi^4} + \frac{\ddot{\psi}^2}{40\Xi^4} + \frac{\dot{\psi}\ddot{\psi}}{240\Xi^4} \right) \mathrm{d}\sigma.\end{aligned}$$

To get the governing equation, we vary the Lagrangian truncated to the second order of $\frac{1}{\Xi}$ with respect to ψ, which gives us the Lagrangian and the equation

$$\mathcal{L} = \int_0^1 \left\{ \Lambda + \frac{1}{\Lambda} + \frac{\dot{\psi}^2}{8\Lambda\Xi^2} + \frac{\mu\cos\psi}{\Lambda} \left(1 + \frac{\dot{\psi}^2}{8\Xi^2} \right) \right\} \mathrm{d}\sigma, \tag{4}$$

$$\ddot{\psi} + \frac{4\mu\Xi^2 \sin\psi}{1 + \mu\cos\psi} \left(1 - \frac{\dot{\psi}^2}{8\Xi^2} \right) = 0. \tag{5}$$

We can also notice that the theory is independent of δ because it is truncated at the second order and the dependence of δ appears only at the fourth order.

Having set up the problem and derived the governing equation (5), we will solve the equation first asymptotically near the buckling threshold and then numerically for bigger compressions. From the problem setup and the variation, boundary conditions arise that we will use for determining of ψ; they are

$$\psi(0) = \psi(1) = 0, \tag{6}$$

$$\int_0^1 \cos\psi \left(1 + \frac{\dot{\psi}^2}{8\Xi^2} \right) \mathrm{d}\sigma = \Lambda(1 - D). \tag{7}$$

The trivial solution that satisfies both the equation and the conditions is $\psi = 0$, $\Lambda = \frac{1}{1-D}$ which corresponds to the flat unbuckled solution of the problem and is the energy minimum for compressions smaller than the buckling threshold.

2.1.3 Solving the governing equation

Having derived the governing equation and found the trivial solution to the problem, we will now solve the equation asymptotically for compressions near the buckling threshold. In order to do that, we introduce a small parameter ϵ such that

$$\epsilon^2 = 1 - \Lambda(1 - D).$$

Furthermore, we expand ψ and the Lagrange multiplier μ as

$$\psi(\sigma) = \epsilon \left[\psi_0(\sigma) + \epsilon\psi_1(\sigma) + \epsilon^2\psi_2(\sigma) + O(\epsilon^3)\right],$$
$$\mu = \mu_0 + \epsilon\mu_1 + \epsilon^2\mu_2 + O(\epsilon^3).$$

We can now plug these expansions into the governing equation (5) and solve it at the different orders of ϵ. At the lowest order (which corresponds to the first order in ϵ), equation (5) boils down to

$$\ddot{\psi_0} + \frac{4\mu_0\Xi^2}{1+\mu_0}\psi_0 = 0.$$

We solve this equation by assuming the solution of the form $e^{\alpha\sigma}$, which gives us the characteristic equation for α,

$$\alpha^2 + \frac{4\mu_0\Xi^2}{1+\mu_0} = 0.$$

This equation gives rise to two solutions of α, $\alpha_{1/2} = \pm i\chi$, where $\chi = 2\Xi\sqrt{\mu_0/(1+\mu_0)}$ and the general solution of the equation is

$$\psi_0 = C_1 \sin(\chi\sigma) + C_2 \cos(\chi\sigma).$$

Using boundary conditions (6) we get $C_2 = 0$ and $\chi = \pi$ in order to get a non-zero solution for ψ. Upon substituting this into the expression for χ, we obtain

$$\boxed{\mu_0 = \frac{z}{1-z}}, \qquad z = \frac{\xi^2}{4}$$

where we have introduced a new variable $\xi = \frac{\pi}{\Xi} \ll 1$ for the sake of convenience. This also gives us the general solution for ψ_0,

$$\boxed{\psi_0(\sigma) = \Psi_0 \sin(\pi\sigma)},$$

where Ψ_0 is a constant which we will determine from the integral condition (7). We continue with the same process for higher orders in ϵ. At the second order in ϵ, the governing equation is

$$\ddot{\psi_1} + \frac{4\Xi^2}{1+\mu_0}(\mu_1\psi_0 + \mu_0\psi_1) = 0.$$

Upon substituting for μ_0 and ψ_0, we get

$$\ddot{\psi_1} + \underbrace{4z\Xi^2}_{\chi^2 = \pi^2}\psi_1 = \underbrace{-4\mu_1(1-z)\Xi^2\Psi_0}_{C}\sin(\pi\sigma).$$

The general solution to this equation is

$$\psi_1(\sigma) = C_1\sin(\pi\sigma) + C_2\cos(\pi\sigma) - \frac{C}{4\pi^2}\left(2\pi\sigma\cos(\pi\sigma + 2\cos^2(\pi\sigma)\sin(\pi\sigma) - \cos(\pi\sigma)\sin(2\pi\sigma)\right).$$

Using boundary conditions (6) we obtain

$$C_2 = 0, \qquad C = 0 \quad \Longrightarrow \quad \boxed{\mu_1 = 0}, \quad \boxed{\psi_1(\sigma) = \Psi_1\sin(\pi\sigma)}.$$

At the third order in ϵ, equation (5) becomes

$$\ddot{\psi_2} + 4z\Xi^2\psi_2 = 4z\Xi^2\left(\frac{\psi_0\dot{\psi_0}^2}{8\Xi^2} - \frac{\psi_0^3}{6}(3z-1)\right) - 4\mu_2\Xi^2(1-z)^2\psi_0.$$

Upon substituting for μ_0 and ψ_0, we get

$$\ddot{\psi_2} + \underbrace{4z\Xi^2}_{\chi^2 = \pi^2} \psi_2 = A\sin(\pi\sigma) + B\sin(3\pi\sigma).$$

where

$$A = \frac{z\pi^2}{8}\Psi_0^3 - \frac{z(3z-1)}{2}\Xi^2\Psi_0^3 - 4\Xi^2\mu_2(1-z)^2\Psi_0, \qquad B = \frac{z\pi^2}{8}\Psi_0^3 + \frac{z(3z-1)}{6}\Xi^2\Psi_0^3.$$

The general solution of this equation is

$$\psi_2 = C_1\cos(\pi\sigma) + C_2\sin(\pi\sigma) - \frac{A\sigma}{2\pi}\cos(\pi\sigma) + \frac{A}{4\pi^2}\sin(\pi\sigma) - \frac{B}{8\pi^2}\sin(3\pi\sigma).$$

Boundary conditions (6) set the constants $C_1 = 0$ and $A = 0$, which gives us both the solutions to μ_2 as well as the solution for ψ_2

$$\boxed{\mu_2 = \left(1 + \frac{\xi^2}{4} - 3z\right)\frac{z\Psi_0^2}{8(1-z)^2}},$$

$$\boxed{\psi_2 = \Psi_2\sin(\pi\sigma) - \frac{B}{8\pi^2}\sin(3\pi\sigma)}.$$

In the next step, we will determine the amplitudes Ψ_0, Ψ_1, and Ψ_2 from the integral condition (7) and get the value of Λ that minimizes the energy.

2.1.4 Calculating the amplitudes

The next step in the analysis is the calculation of the amplitudes Ψ_0, Ψ_1, and Ψ_2, which we will get from the integral condition (7). Using the definition of ϵ, as well as the expansion of ψ in ϵ, we expand both sides of this condition and get the amplitudes from comparing the expansions on the left and on the right at different orders of ϵ. This analysis yields

$$\Psi_0 = \frac{2}{\sqrt{1-z}}, \qquad \Psi_1 = 0, \qquad \Psi_2 = \frac{4(2-\xi^2)}{(4-\xi^2)^{\frac{5}{2}}}.$$

2.1.5 The buckling condition

Similarly to Ref. [2], upon minimizing the energy and substituting for Λ from the definition of ϵ, the energy takes the form

$$E = \left(\frac{1}{1-D} + 1 - D\right) + \left(\frac{1-D}{1-z} - \frac{1}{1-D}\right)\epsilon^2 + O(\epsilon^3).$$

The expression in the first set of parentheses corresponds to the energy of the monolayer for the trivial solution $\psi = 0$, $\Lambda = (1-D)^{-1}$. Therefore we can extract the buckling threshold from the condition that the term of order ϵ^2 should be less than zero, which would mean that the buckled configuration is more favorable in this case. This implies

$$\frac{1-D}{1-z} - \frac{1}{1-D} < 0 \Longrightarrow D > D_* = 1 - \sqrt{1-z}.$$

The last step in the buckling analysis is determining the value of Λ that minimizes the energy of the buckled configuration. In order to do this, we relate ϵ to the relative compression $d = D - D_*$ by writing $\epsilon = \epsilon_0 d^{1/2} + O(d)$, which then allows us to expand the energy in terms of d,

$$E = \frac{8-\xi^2}{2\sqrt{4-\xi^2}} - \frac{\xi^2}{\xi^2-4}d + \frac{8(4-\xi^2) - 8\epsilon_0^2(4-\xi^2-4)^{3/2} + \epsilon_0^4(32-14\xi^2+\xi^4)}{(4-\xi^2)^{5/2}}d^2 + O(d^3).$$

Finding the derivative of the energy with respect to ϵ_0, and setting it to be equal to zero, gives us the expression for ϵ_0,

$$\epsilon_0 = \frac{2\sqrt{4-\xi^2}}{\sqrt{32-14\xi^2+\xi^4}}.$$

The next step is to investigate the folding caused by compressions $D > D_*$ numerically. Also, we will introduce another behaviour, namely the transition to constricted cells. During the folding process, the individual cells fold more and more until they assume a triangular shape. Beyond this point, the lateral sides of individual cells would intersect. At the continuum level, this would mean that the monolayer of the epithelium would start to self-intersect, which we empirically know does not happen. This phenomenon then imposes another condition when reaching higher compressions. To solve the equation at this point of the buckling process, one has to look at the constricted cells which are triangular separately from the rest of the cell sheet.

2.1.6 Estimate of $D_\triangle$

In order to investigate the buckling behaviour, the coordinates of the midline are calculated using Eqs. (2) and (3). The coordinates of the apical and basal sides are then

$$x_\pm = x \mp \frac{l}{2}\sin\psi, \qquad y_\pm = y \pm \frac{l}{2}\cos\psi, \tag{8}$$

where $l = l_0\Lambda\cos\phi$ is the local cell sheet thickness. This enables us to plot the shape of the cell sheet as a result of the compression, which can be seen in Fig. 4.

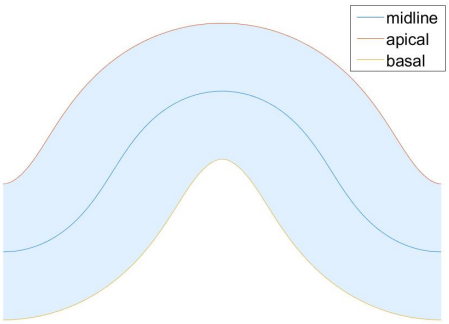

Figure 4: The shape of the cell sheet as a response to the compression.

We then increase the compression and solve the governing equations (5), along with conditions (6) and (7) using MATLAB's boundary value problem solver bvp4c. The unknown parameter μ is also a result of the solver, while the value of Λ which minimizes the energy is obtained in the following way: the system is solved for a set of values of Λ and then the energy of the system is calculated using the solutions of ψ and Λ. Then the energy is minimized and the solutions that correspond to this minimum are the solutions of ψ and Λ that are taken into account.

By solving the equation numerically, we can infer the threshold $D_\triangle$ at which the self-intersection arises. From the numerics we can also see that the self-intersection takes place for $\sigma = 0$ first, when $\dot{x}_+ = 0$ which we can use as a rough estimate of $D_\triangle$. Taking the derivative with respect to σ of the expression for x_+ given in Eq. (8), and setting $\sigma = 0$, using Eqs. (1) and (2) we obtain

$$\frac{f(0)}{\Lambda} - \Lambda\frac{l_0^2}{2\Xi}\dot{\psi}(0)\cos\phi(0) = 0 \tag{9}$$

From the definition of ϵ, we can express Λ as $\Lambda = (1-\epsilon^2)(1-D)^{-1}$. Now using the expansion $\epsilon = \epsilon_0\sqrt{d} + O(d)$, we obtain the expansion of Λ in terms of the relative compression in the form $\Lambda = (1-D_*)^{-1} + O(d) = (1-z)^{-1/2} + O(d)$. Plugging that into the previous expression and solving it for d gives us the estimate

$$d \approx \frac{r^2}{\pi^2},$$

where $r = \Xi/l_0^2$ is introduced for the sake of convenience. Since $D_\triangle \gg D_* \approx 0.003$, the previous approximation gives us a rough estimate of $D_\triangle \approx r^2/\pi^2$, which coincides quite well with the results obtained from the numerics as seen in Fig. 5, where we can empirically tell when the self-intersection takes place.

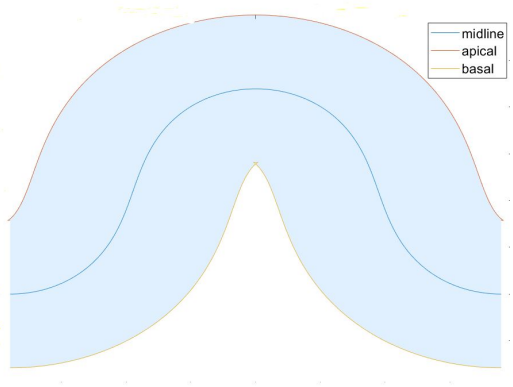

Figure 5: The numerical solution for $\Xi = 20$, $l_0 = \sqrt{10}$, $D = 0.4 = \frac{r^2}{\pi^2}$.

2.1.7 Numerical solution of the governing equation for $D > D_\triangle$

Since the asymptotic expansion is consistent only for compressions just above the buckling threshold, we solve Eq. (5) for bigger compression numerically in MATLAB, using the numerical solver bvp4c. For the initial guess we input the solution for the asymptotic problem as well as give it an initial guess for $\mu = 0.006$, which corresponds to the analytical value of μ. Then the equation is solved for a number of values of Λ, with the help of the boundary conditions (6) and the displacement condition (7). Then the energy of the system is calculated for the numerical solution of ψ and the input value of Λ, using

$$E = \int_0^1 \left(\Lambda + \frac{1}{\Lambda} + \frac{\dot{\psi}^2}{8\Lambda\Xi^2} \right) \mathrm{d}\sigma.$$

The code then plots the dependence of the energy on the value of Λ used in the solving of Eq. (5), finds the value of the minimum of that function and then finally solves the equation Eq. (5) for the value of Λ that minimizes the energy.

2.1.8 Redefining the solving of the governing equation for $D > D_\triangle$

In order to investigate the buckling for compressions larger than $D_\triangle$, we introduce a new variable s_* which tracks the position of the constricted cells. Since the buckled configuration has a symmetry even on the interval $\sigma \in [0, 1]$, we can simplify the problem by solving the governing equation for $\sigma \in [0, \frac{1}{2}]$. Since the numerics revealed that the constricted cells first emerge around $\sigma = 0$, we divide the domain of σ into two segments: $\sigma \in [0, s_*]$ where the constricted cells which can no longer fold are and $\sigma \in [s_*, \frac{1}{2}]$ where the cells can continue to fold. We begin the analysis by introducing a new parametrization of the problem via

$$\sigma = s_* + (1 - 2s_*)\sigma',$$

with the goal of redefining the equation and the conditions in terms of the new variable $\sigma' \in [0, \frac{1}{2}]$ which describes the segment of the cell sheet corresponding to $\sigma \in [s_*, \frac{1}{2}]$. This is where the folding continues, while for the $\sigma \in [0, s_*]$, we already know the solution from the numerical solving for $D < D_\triangle$ and this is the solution used for this part of the domain, since we assumed this is where the triangular cells are. The redefinition of the parametrization affects both the governing equation, as well as the boundary conditions.

In order to do this consistently, we return to the definition of the Lagrangian of the system (4) and as a first step use the symmetry around $\sigma = \frac{1}{2}$ to reduce the range of integration to $\sigma \in [0, \frac{1}{2}]$.

The condition that the buckling is symmetric around $\sigma = \frac{1}{2}$ is

$$\psi(\sigma) = \psi(1-\sigma) \Longrightarrow \dot{\psi}(\sigma) = -\dot{\psi}(1-\sigma).$$

Splitting the integration into $[0, \frac{1}{2}]$ and $[\frac{1}{2}, 1]$ and introducing a new variable $\sigma_1 = 1-\sigma$ into the second integral, we see that the second integral is equal to the first one, so the Lagrangian is just

$$\mathcal{L} = 2\int_0^{\frac{1}{2}} \left\{ \Lambda + \frac{1}{\Lambda} + \frac{\dot{\psi}^2}{8\Lambda\Xi^2} + \frac{\mu\cos\psi}{\Lambda}\left(1 + \frac{\dot{\psi}^2}{8\Xi^2}\right) \right\} \mathrm{d}\sigma.$$

For $\sigma \in [0, s_*]$, we know the numerical solution for ψ and $\dot{\psi} \overset{\text{def}}{=} \dot{\psi}_{max}$, while for $\sigma \in [s_*, \frac{1}{2}]$, we assume $\dot{\psi} = \dot{\psi}_{max} - \Psi^2$ and vary the Lagrangian with respect to Ψ to get the new equation. This variation yields the same equation as (5) as a function of σ. We then rewrite the equation in terms of σ',

$$\frac{1}{(1-2s_*)^2}\frac{d^2\psi}{d\sigma'^2} + \frac{4\mu\Xi^2\sin\psi}{1+\mu\cos\psi}\left[1 - \frac{1}{8\Xi^2(1-2s_*)^2}\left(\frac{d\psi}{d\sigma'}\right)^2\right] = 0.$$

The boundary conditions are

$$\dot{\psi}(\sigma) = -\dot{\psi}(1-\sigma) \Longrightarrow \dot{\psi}\left(\frac{1}{2}\right) = 0, \qquad \psi(0) = \dot{\psi}_{max} s_*,$$

where the first condition comes from the symmetry of the system, and the second one comes from the continuity condition for ψ at $\sigma = s_*$. Furthermore, another condition is needed in order to obtain the value of s_* which depends on the compression and can be calculated by varying the energy with respect to s_*. The energy of the system is

$$E = 2\int_0^{\frac{1}{2}} \left(\Lambda + \frac{1}{\Lambda} + \frac{\dot{\psi}^2}{8\Lambda\Xi^2}\right)\mathrm{d}\sigma = 2\int_0^{s_*} \left(\Lambda + \frac{1}{\Lambda} + \frac{\dot{\psi}_{max}^2}{8\Lambda\Xi^2}\right)\mathrm{d}\sigma + 2\int_{s_*}^{\frac{1}{2}} \left(\Lambda + \frac{1}{\Lambda} + \frac{\dot{\psi}^2}{8\Lambda\Xi^2}\right)\mathrm{d}\sigma.$$

Varying this expression with respect to s_* gives

$$\delta E = 2\left[\frac{\dot{\psi}_{max}^2(s_*^-)}{8\Lambda\Xi^2} - \frac{\dot{\psi}^2(s_*^+)}{8\Lambda\Xi^2}\right]\delta s_* = 0 \quad \Longrightarrow \quad \dot{\psi}(0) = \dot{\psi}_{max}.$$

We can determine the value of $\dot{\psi}_{max}$ from the condition of self-intersection, Eq. (9). Using

$$f(0) = 1 + \frac{\dot{\psi}^2(0)}{24\Xi^2}, \qquad \phi(0) = \frac{\dot{\psi}(0)}{2\Xi},$$

expanding $\cos\phi(0)$ and substituting $\dot{\psi}(0) = \dot{\psi}_{max}$, we obtain a cubic equation for $\dot{\psi}_{max}$,

$$l_0^2\frac{\Lambda}{16\Xi^3}\dot{\psi}_{max}^3 + \frac{1}{24\Lambda\Xi^2}\dot{\psi}_{max}^2 - \frac{l_0^2}{2\Xi}\Lambda\dot{\psi}_{max} + \frac{1}{\Lambda} = 0.$$

Since the theory is truncated at order $O(\frac{1}{\Xi^2})$, we discard the cubic term and solve the quadratic equation for $\dot{\psi}_{max}$, and obtain

$$\dot{\psi}_{max} = \frac{\Xi}{2}\left(3l_0^2\Lambda^2 - \sqrt{9l_0^4\Lambda^4 - 24}\right).$$

Lastly, the displacement condition (7) is first simplified by integrating up to $\frac{1}{2}$ because of the mentioned symmetry, which only gives a factor of $\frac{1}{2}$ in front of the right side of the expression,

$$\int_0^{\frac{1}{2}} \cos\psi\left(1 + \frac{\dot{\psi}^2}{8\Xi^2}\right)\mathrm{d}\sigma = \frac{1}{2}\Lambda(1-D).$$

Next we split the integration at s_*, where we know that $\psi = \dot{\psi}_{max}\sigma$ for $\sigma \in [0, s_*]$. Plugging this in, we can integrate the expression for $\sigma \in [0, s_*]$, and then introduce σ' in the remaining integrand, which ultimately gives us the following condition:

$$\int_0^{\frac{1}{2}} \cos\psi(\sigma') \left[1 + \frac{1}{8\Xi^2(1-2s_*)^2}\left(\frac{d\psi}{d\sigma'}\right)^2\right](1-2s_*)\,\mathrm{d}\sigma' = \frac{1}{2}\Lambda(1-D) - \left(1 + \frac{\dot{\psi}_{max}^2}{8\Xi^2}\right)\frac{\sin\left(\dot{\psi}_{max}s_*\right)}{\dot{\psi}_{max}}.$$

We then solve the governing equation numerically with these new conditions, compute the energy of the system and determine the value of Λ that minimizes the energy as before.

2.1.9 Results

We can now run the code for different values of the compression D, where for compressions larger than $D_\triangle$ the governing equation is solved with the modifications derived above. We can then plot the dependence of Λ and μ on the compression for different values of Ξ.

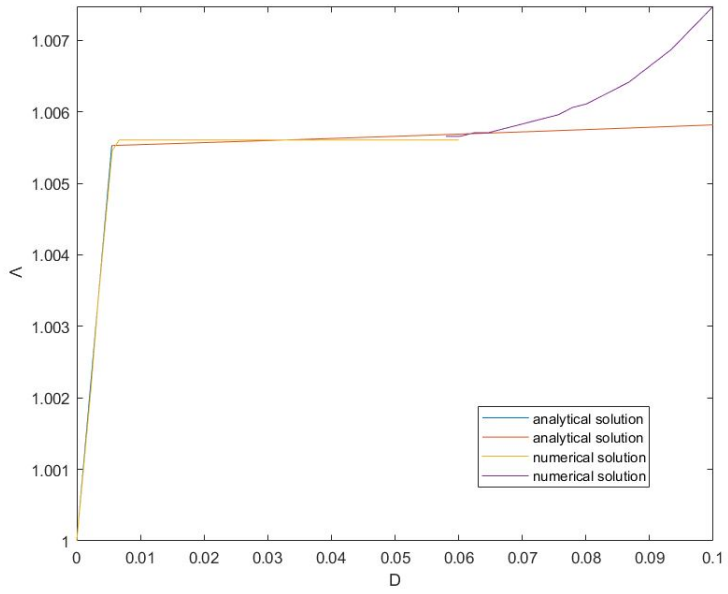

(a) The dependence of Λ on the compression D.

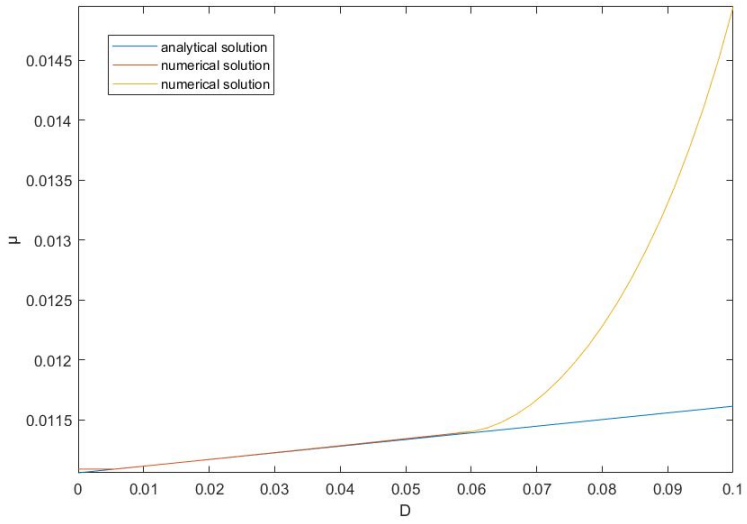

(b) The dependence of μ on the compression D.

Figure 6: Results of the numerical solution for $\Xi = 15$, $l_0 = \sqrt{20}$.

As can be seen in Figs. 6 and 7, the numerical results agree quite well with the analytical ones, up to the compression of $D_\triangle$. For $D > D_\triangle$ we can see the value of μ, which can be interpreted as a horizontal, compressive force in the sheet rises sharply in both of the depicted scenarios. Concerning Λ, we have depicted here two possible cases, where again the results align with the analytical ones up until $D_\triangle$. However there is an increase of Λ in the first case and a steep decrease in the other. Since Λ is the thickness of the sheet relative to the thickness in the flat configuration, we can see that for $D < D_*$ there is a sharp jump for Λ, which is the regime in which the sheet is in its flat configuration, therefore it makes up for the compression by increasing the thickness of the sheet rapidly. After the bending of the cell sheet starts, Λ hits a plateau, and for $D > D_\triangle$, we can see another rapid change in the thickness as a result of the presence of the constricted cells.

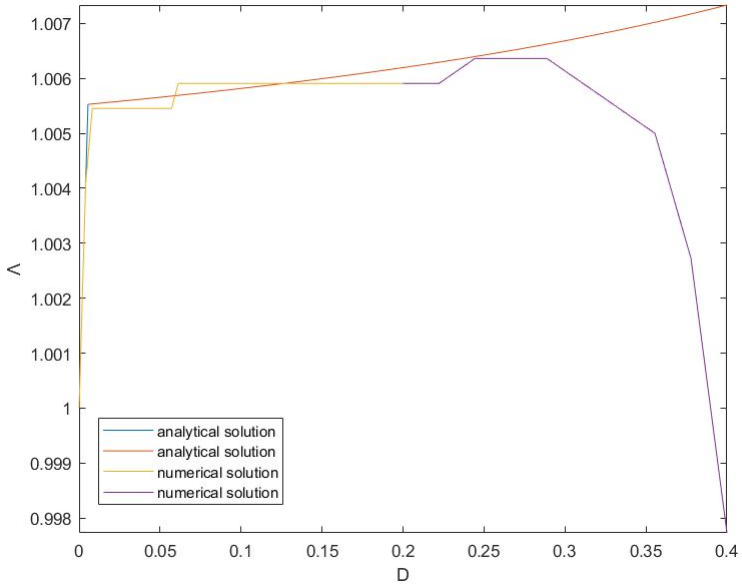

(a) The dependence of Λ on the compression D.

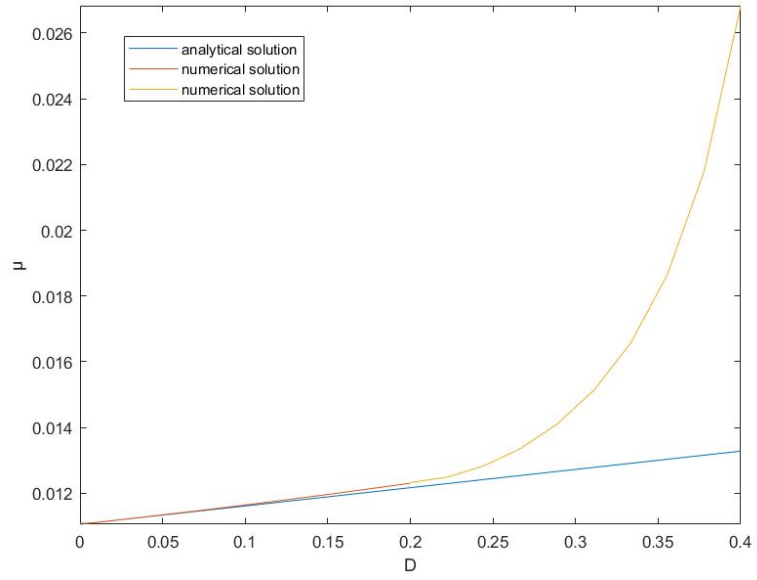

(b) The dependence of μ on the compression D.

Figure 7: Results of the numerical solution for $\Xi = 15$, $l_0 = \sqrt{10}$.

2.2 Non-isosceles monolayer

In the next step, we want to relax our starting assumption of the shape of the individual cells being isosceles trapezoids. We now assume that the cells become non-isosceles trapezoids while bending, which we can then describe using two angles ϕ and θ. We also introduce the thickness of the individual

cells in order to describe the continuum model, as shown in Fig. 8.

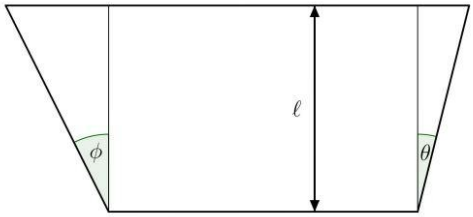

Figure 8: Describing the non-isosceles trapezoids. Taken from Ref. [3].

In order to derive the continuum model following Ref. [3], we use the shared-wall constraint, which guarantees that the lateral sides of the sides match up, as shown in Fig. 9.

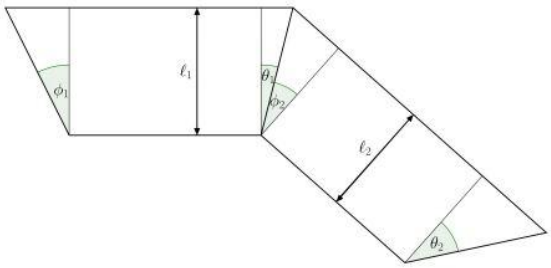

Figure 9: The shared-wall condition. Taken from Ref. [3].

As we can see from the above figure, this condition can be expressed as

$$\frac{l_i}{\cos\theta_i} = \frac{l_{i+1}}{\cos\phi_{i+1}}. \tag{10}$$

The geometry of the system gives rise to the expression that gives us the connection between the cell level variables and continuous variables, as in Ref. [3]:

$$\theta(s) + \phi(s+s_0) = \frac{\psi'(s)}{l_0} + \frac{\psi''(s)}{2l_0^2} + \frac{\psi'''(s)}{6l_0^3} + \frac{\psi^{(iv)}(s)}{24l_0^4} + \frac{\psi^{(v)}(s)}{120l_0^5}. \tag{11}$$

We then introduce an epithelium-level variable $z(s)$ by writing

$$\frac{l(s)}{l_0} = \zeta + \frac{z(s)}{\Xi}, \tag{12}$$

where $l(s)$ is the thickness of the epithelium monolayer which is now a function of the position and not a constant as it was in the previous case. Here, ζ is the relative thickness of the cell sheet right before the folding starts, since we know from the previous analysis that up to the buckling threshold of the compression, the sheet is in the flat configuration, which results in a rapid increase of the thickness of the cell sheet.

We can then plug Eq. (12) into Eq. (10), with l_i corresponding to $l(s)$ in the continuum model, l_{i+1} to $l(s+s_0)$, θ_i to $\theta(s)$ and ϕ_{i+1} to $\phi(s+s_0)$. Similarly, we plug in $\phi(s+s_0)$ from Eq. (11), and then expand the right-hand side around s, which ultimately gives us the dependence of θ on the continuum-level variables z and ψ,

$$\theta = \underbrace{\frac{1}{\Xi}\left(\frac{\dot\psi}{2} + \frac{\dot z}{\zeta\dot\psi}\right)}_{\theta_0(\sigma)} + \underbrace{\frac{1}{\Xi^2}\left(\frac{\ddot\psi}{4} - \frac{\dot z\ddot\psi}{2\zeta\dot\psi^2} + \frac{\ddot z}{2\zeta\dot\psi} - \frac{z\dot z}{\zeta^2\dot\psi}\right)}_{\theta_1(\sigma)} + O\left(\frac{1}{\Xi^3}\right).$$

Based on the expansion of θ in $\frac{1}{\Xi}$, we can assume a similar one for ϕ,

$$\phi(\sigma) = \frac{1}{\Xi}\phi_0(\sigma) + \frac{1}{\Xi^2}\phi_1(\sigma) + O\left(\frac{1}{\Xi^3}\right).$$

We then plug this assumed expansion for ϕ, as well as the obtained one for θ into Eq. (11), while expanding $\phi(s+s_0)$ around s. Comparing terms on both sides, order-by-order in $\frac{1}{\Xi}$, we get

$$\phi = \frac{1}{\Xi}\underbrace{\left(\frac{\dot{\psi}}{2} - \frac{\dot{z}}{\zeta\dot{\psi}}\right)}_{\phi_0(\sigma)} + \frac{1}{\Xi^2}\underbrace{\left(-\frac{\ddot{\psi}}{4} - \frac{\dot{z}\ddot{\psi}}{2\zeta\dot{\psi}^2} + \frac{\ddot{z}}{2\zeta\dot{\psi}} + \frac{z\dot{z}}{\zeta^2\dot{\psi}}\right)}_{\phi_1(\sigma)} + O\left(\frac{1}{\Xi^3}\right).$$

Then we can easily obtain the energy of the system by plugging in these two expansions that link the cell-level variables with the continuum variables in the energy density, as in Ref. [3],

$$e(s) = \frac{l_0^2}{l(s)} + l(s)\left(\delta\frac{\tanh\phi(s) + \tan\theta(s)}{2} + \frac{\sec\theta(s) + \sec\phi(s)}{2}\right)$$

In order to define the Lagrangian of the system we still need to obtain the displacement condition, which we again obtain from the geometry of the system. Similarly to Ref. [2],

$$x(s+s_0) - x(s) = \frac{1}{2}\left[\kappa(s)\cos\psi(s) + \kappa(s+s_0)\cos\psi(s+s_0)\right],$$

where $\kappa(s)$ is the nondimensionalized length of the midline,

$$\kappa(s) = \frac{1}{l(s)} = \frac{1}{l_0\left(\zeta + \frac{z(s)}{\Xi}\right)}.$$

Using that, we can expand both sides of the expression around s up to order $\frac{1}{\Xi^2}$, and assuming the expansion $\dot{x} = x_0 + \frac{x_1}{\Xi} + \frac{x_2}{\Xi^2} + O(\frac{1}{\Xi^3})$ and again comparing terms on both sides order-by-order in $\frac{1}{\Xi}$, we obtain

$$\dot{x} = \frac{\Sigma}{\zeta}\cos\psi - \frac{1}{\Xi}\frac{\Sigma}{\zeta^2}z\cos\psi + \frac{1}{\Xi^2}\left(\frac{\Sigma}{\zeta^3}z^2\cos\psi - \frac{\Sigma}{3\zeta}\cos\psi\right).$$

We can finally plug in both the energy and the displacement condition into the Lagrangian of the system,

$$\mathcal{L} = E + \frac{\mu}{\Sigma}\int_0^1 \dot{x}(\sigma)\,\mathrm{d}\sigma.$$

After integrating out the terms that are equal to zero as a consequence of the imposed boundary conditions, we get

$$\mathcal{L} = \int_0^1 \left\{\left(\frac{1}{\zeta} + \zeta\right) + \frac{z}{\Xi}\left(1 - \frac{1}{\zeta^2}\right) + \frac{1}{\Xi^2}\left(\frac{z^2}{\zeta^3} + \frac{\delta z\dot{\psi}}{2} + \frac{\dot{z}^2}{2\zeta\dot{\psi}^2} + \zeta\frac{\dot{\psi}^2}{8}\right)\right\}\mathrm{d}\sigma$$
$$+ \frac{\mu}{\zeta}\int_0^1 \cos\psi\left[1 - \frac{z}{\zeta\Xi} + \frac{1}{\Xi^2}\left(\frac{z^2}{\zeta^2} - \frac{1}{3}\right)\right]\mathrm{d}\sigma.$$

Varying this Lagrangian with respect to ψ and z yields the equations

$$\boxed{2\Xi\zeta\left(1 - \frac{1}{\zeta^2}\right)\dot{\psi}^3 + \frac{4z\dot{\psi}^3}{\zeta^2} + \delta\zeta\dot{\psi}^4 - 2\ddot{z}\dot{\psi} + 4\dot{z}\ddot{\psi} + 2\mu\cos\psi\dot{\psi}^3\left(-\frac{\Xi}{\zeta} + \frac{2z}{\zeta^2}\right) = 0},$$

$$\boxed{2\delta\zeta\dot{z}\dot{\psi}^4 - 8\dot{z}\ddot{z}\dot{\psi} + 12\ddot{\psi}\dot{z}^2 + \zeta^2\ddot{\psi}\dot{\psi}^4 + 4\mu\sin\psi\dot{\psi}^4\left[\Xi^2 - \frac{z}{\zeta}\Xi + \left(\frac{z^2}{\zeta^2} - \frac{1}{3}\right)\right] = 0},$$

that we should solve, while imposing the conditions $\psi(0) = \psi(1) = 0$ and $\dot{z}(0) = \dot{z}(1) = 0$, as well as

$$\frac{\mu}{\zeta}\int_0^1 \cos\psi \left[(]1 - \frac{z}{\zeta\Xi} + \frac{1}{\Xi^2}\left(\frac{z^2}{\zeta^2} - \frac{1}{3}\right)\right] \mathrm{d}\sigma = 1 - D.$$

We then tried to solve these equations around the buckling threshold, assuming the scalings

$$\psi(\sigma) = \epsilon\left[\psi_0(\sigma) + \epsilon\psi_1(\sigma) + \epsilon^2\psi_2(\sigma)\right] + O(\epsilon^4),$$
$$z(\sigma) = z_0(\sigma) + \epsilon z_1(\sigma) + \epsilon^2 z_2(\sigma) + O(\epsilon^3).$$

However, plugging these expansions into the equations along with the expansions of ζ and μ results in very complicated equations already at the lowest order in ϵ.

3 Conclusion

The goal of the project was to derive a continuum theory that would successfully explain the folding of a cell sheet as a result of compression applied to the sides of the sheet, as well as different surface tensions acting on the sides of the cells.

Using the initial assumption that individual cells can be described as isosceles trapezoids for developing a continuum model of a cell sheet seems to give us a fairly simple continuum theory that explains the buckling of the cell sheet even for large compressions. Qualitatively, we can observe three regimes:

(1) For $D \in [0, D_*]$ the flat solution is energetically favorable, so the system stays in the flat configuration, making up for the compression of the sides by increasing the thickness of the sheet.

(2) For $D \in [D_*, D_\triangle]$ the cell sheet begins to fold.

(3) For $D \in [D_\triangle, 1]$ at certain points of the sheet individual cells form triangular cells, whereas the rest of the sheet continues to fold.

We have successfully determined both of the thresholds D_* and $D_\triangle$ and have been able to describe the configuration of the monolayer for all compressions.

However, once we relax the initial assumption and try to develop the theory by assuming that the shape of the cells during folding can be described by non-isosceles trapezoids, the theory quickly becomes very complicated and hard to solve even around the buckling threshold. This might suggest that the first model may be too simple to describe the buckling process well.

References

[1] Anastasiya et al Trushko. Buckling of an epithelium growing under spherical confinement. *Developmental Cell*, 54(5):655–668.e6., 2020 Sep 14.

[2] Pierre A. Haas and Raymond E. Goldstein. Nonlinear and nonlocal elasticity in coarse-grained differential-tension models of epithelia. *Phys. Rev. E*, 99:022411, Feb 2019.

[3] Marcin Pruszczyk and Pierre Haas. Continuum mechanics of epithelial mono- and bilayers. Oct 2021.